



**HAL**  
open science

# Design of thermochemical heat transformer for waste heat recovery: Methodology for reactive pairs screening and dynamic aspect consideration

Benoit Michel, Marc Clause

## ► To cite this version:

Benoit Michel, Marc Clause. Design of thermochemical heat transformer for waste heat recovery: Methodology for reactive pairs screening and dynamic aspect consideration. *Energy*, 2020, pp.118042. 10.1016/j.energy.2020.118042 . hal-02929385

**HAL Id: hal-02929385**

**<https://hal.science/hal-02929385v1>**

Submitted on 3 Sep 2020

**HAL** is a multi-disciplinary open access archive for the deposit and dissemination of scientific research documents, whether they are published or not. The documents may come from teaching and research institutions in France or abroad, or from public or private research centers.

L'archive ouverte pluridisciplinaire **HAL**, est destinée au dépôt et à la diffusion de documents scientifiques de niveau recherche, publiés ou non, émanant des établissements d'enseignement et de recherche français ou étrangers, des laboratoires publics ou privés.

# Design of Thermochemical Heat Transformer for Waste Heat Recovery: methodology for reactive pairs screening and dynamic aspect consideration

Benoit Michel<sup>a,\*</sup>, Marc Clausse<sup>a</sup>

<sup>a</sup>Univ. Lyon, CNRS, INSA Lyon, CETHIL, UMR5008, Villeurbanne, F-69621, France, Université Lyon 1, F-69622, France

---

## Abstract

Waste Heat Recovery in the industrial sector often requires to upgrade the temperature of the heat fluxes in order to make them useful for the process. Thermochemical Heat Transformer (THT) and especially 2-salt configuration, can play a major role as they can achieve high temperature lift when compared to alternative technologies. Despite various developments in recent years, this technology still suffers from several issues to make it fully attractive: rapid and reliable reactive salt selection, heat and mass transfer intensification, coupling with process heat demand, etc.

This work is focused on a new methodology to achieve a rapid screening of salt pairs for a given application (i.e. source temperatures). Four criteria, based on thermodynamic considerations, are proposed allowing for an example to go from 4290 possibilities to only three most promising pairs at the end.

A second part is dedicated to dynamic aspect considerations, exploring the robustness of the solution towards changes in heat transfer and kinetic coefficients as well as to changes in heat source temperatures. Knowledge on this last aspect is of great importance to achieve efficient integration to cover process heat demand.

### Keywords:

Thermochemical Heat Transformer, Waste Heat, Salt screening

---

## Nomenclature

$c$  heat capacity,  $\text{J kg}^{-1} \text{K}$

$COP$  coefficient of performance, (-)

$F_m$  driving force, (-)

$G$  reactive gas, (-)

$k_{cin}$  kinetic constant,  $\text{s}^{-1}$

$M$  molar weight,  $\text{kg mol}^{-1}$

$m$  mass,  $\text{kg}$

$\dot{m}_v$  sink or source of gas,  $\text{kg s}^{-1}$

$\dot{m}$  mass flow rate,  $\text{kg s}^{-1}$

$p$  pressure,  $\text{Pa}$

$P_m$  specific power,  $\text{W kg}^{-1}$

$\dot{q}$  sink or source of heat,  $\text{W s}^{-1}$

$Q$  heat exchange,  $\text{J}$

$R$  ideal gas constant,  $\text{J mol}^{-1} \text{K}^{-1}$

$S$  dehydrated reactive solid, (-)

$S'$  hydrated reactive solid, (-)

$T$  temperature,  $\text{K}$  or  $^{\circ}\text{C}$

$UA$  heat exchange coefficient,  $\text{W m}^{-2} \text{K}^{-1}$

$X$  reaction advancement, (-)

### Greek symbols

$\Delta g_r$  free Gibbs energy,  $\text{J mol}^{-1}_s$

$\Delta h_r^0$  standard enthalpy of reaction,  $\text{J mol}^{-1}_v$

$\Delta s_r^0$  standard entropy of reaction,  $\text{J K}^{-1} \text{mol}^{-1}_v$

$\nu$  stoichiometric coefficient,  $\text{mol}_v \text{mol}^{-1}_s$

### Indices

---

\*Corresponding author

E-mail: benoit.michel@insa-lyon.fr (B. Michel)

<i>eq</i> solid/gas equilibrium	<i>max</i> maximum
<i>exch</i> exchanger	<i>n</i> HT or LT salt
<i>i</i> inlet	<i>o</i> outlet
<i>htf</i> heat transfer fluid	<i>s</i> salt
<i>H</i> high temperature	<i>v</i> vapor
<i>HT</i> high temperature salt	
<i>L</i> low temperature	
<i>LT</i> low temperature salt	<i>Exponents</i>
<i>m</i> medium	<i>o</i> reference

## 1. Introduction

Waste heat valorization is a promising solution to dramatically increase the energy efficiency of the industrial sector. As reported by Forman et al. [1], a huge amount of waste heat is available in this sector. At the world scale 8 861 TWh/year are lost of which 42% at low temperature (<100°C). Thus, there is a big potential for reducing costs and increasing efficiencies in this sector. However, the too low temperature level to satisfy process requirements and the phase shift to the heat demand are the two main drawbacks to the implementation of processes for the re-use of industrial waste heat. To overcome these problems, several solutions such as heat storage and heat to heat conversion systems (heat pumps and heat transformers) have been studied in the last years [2–4].

Among the systems of heat to heat conversion, three technologies are currently being considered: Electrical heat pump (EHP), heat transformers (Absorption heat transformer (AHT) and Thermochemical heat transformer (THT)). Electrical heat pump (EHP) has shown promising results in industrial heat recovery applications, but it still suffers from various drawbacks: high price ratio of electricity to fossil fuel, limited high temperature (EHP available on market deliver heat at 130 °C at maximum), the lack of available refrigerants in the high temperature range with low GWP [4]. Furthermore, process integration might require to store heat to handle variations in supply or demand, which is only feasible by adding a dedicated heat storage while AHP and THT can deliver heat storage service to the process without adding an extra component [5].

AHT and THT use the heat involved by a reversible sorption reaction between a gas and: a liquid for AHT (absorption reaction), a solid for THT (chemical reaction). Moreover, despite a low thermal COP (around 0.5 for a single-stage configuration), these systems present the advantage to not consume electricity. Among the two main technologies of heat transformers, AHT has been the most studied these last years. Although promising, these systems present several issues, as corrosion problems and use of complex cycles to achieve a high temperature lift (>40 K) [6]. Compared to the EHP and AHT, THT is a far less mature technology: there have been few studies on reactive pairs and only few experimental studies [7–13]. However, this technology could potentially tackle the issues of EHP and AHT by achieving both high temperature lift (>50 K) and delivered heat temperature, with 1-stage heat driven system and no crystallization or corrosion problems [5]. Furthermore, the 2-salt technology, also called resorption heat pump, allows to reduce the high pressure lift occurring in sorption heat transformer when high temperature [14].

Among the operating cycles of THT, the 1-salt and 2-salt rings are the two main configurations [8]. In the 1-salt cycle, the system consists of two reactors alternately connected to an evaporator and a condenser (see fig. 1a). The 2-salt technology (fig. 1b), also called resorption heat pump, allows a reduction of the high-pressure lift occurring in heat transformer when high temperature lifts are sought [8]. In this case, the evaporator and the condenser are replaced by two reactors filled with a so-called low temperature salt (LT salt). In the 2-salt systems, the management of the operating pressures, which condition the temperature lift, can be problematic considering the differences in reaction rates of the two reactive salts [14]. Particular attention must be paid to the dynamics evolution of such systems [6].

Furthermore, a main issue of such systems is to select the appropriate salt pair for given operating temperatures ( $T_L$ ,  $T_m$  &  $T_H$ ), to achieve high performance. There exist a large number of solid-gas working pairs.

Many considerations can be taken into account for pair selection: heat of reaction, thermal conductivity, thermal stability, toxicity, cost, etc. Salt/ammonia pairs have been extensively studied for THT applications while there have been some evaluation of salt/methanol, salt/H<sub>2</sub>O and salt/CO<sub>2</sub> pairs with encouraging results for the last two [8]. Among these couples, those using water vapor as reactive gas seem to be ideal for THT applications for industry (low cost, non-toxicity). Thus, Richter et al. [13] identified promising pairs (especially SrBr<sub>2</sub>/H<sub>2</sub>O) for 1-salt THT and for thermal upgrade temperature between 150 to 300 °C (from a screening of 308 salt/H<sub>2</sub>O couples). However, nowadays no screening has been done for 2-salt THT. In these systems, using two reactive pairs coupled, the choice of the reactive couples strongly influences the performances.

This paper proposes a methodology to identify the best salt pairs for THT using water as working fluid for industrial waste heat recovery applications. The scope is to be able to deliver heat at 150 °C, at least. Indeed, this temperature level corresponds to utility temperature levels (steam generation) that are encountered in many industries: agro-food, chemistry, dyeing, etc. For this aim, a two-step approach is proposed:

1. a salt screening for industrial waste heat upgrade (from <100°C to 150°C and above) thanks to a static thermodynamic approach
2. an assessment the impact of the dynamic behavior on THT performance for selected pairs in step 1, thanks to an original model, which is presented and validated in this paper.

## 2. Static thermodynamic approach for salt selection

### 2.1. Solid/gas thermochemical process

The thermochemical heat transfer is based on the thermal effect of a monovariant reversible reaction between a solid and a gas. In this paper only hydrate/water pairs are studied.



The equilibrium conditions ( $p_{eq}$ ,  $T_{eq}$ ) of the solid/gas reaction follow the Clausius-Clapeyron relation, obtained by stating that the free Gibbs energy of the transformation is equal to zero at the thermodynamic equilibrium. Assuming the reactive gas as perfect gas, the free Gibbs energy writes:

$$\Delta g_r = \Delta g_r^0 + RT_{eq} \ln \left( \frac{p_{eq}}{p^0} \right)^\nu = \nu \Delta h_r^0 - \nu T_{eq} \Delta s_r^0 + RT_{eq} \ln \left( \frac{p_{eq}}{p^0} \right)^\nu = 0 \quad (2)$$

$p^0$  is the reference pressure (1 bar),  $\Delta h_r^0$  and  $\Delta s_r^0$  are respectively the standard enthalpy and entropy of reaction and  $\nu$  is the stoichiometric coefficient.

Finally, the thermodynamic equilibrium conditions are determined by only one intensive variable (the equilibrium pressure,  $p_{eq}$ , or the equilibrium temperature,  $T_{eq}$ ):

$$p_{eq} = p^0 e^{\frac{-\Delta h_r^0}{RT_{eq}} + \frac{\Delta s_r^0}{R}} \quad (3)$$

### 2.2. Operating of thermochemical heat transformers

Among the operating cycles of THT using water as reactive gas, the 1-salt and 2-salt rings are the two main configurations [8].

In the 1-salt cycle, the system consists of two reactors alternately connected to an evaporator and a condenser (see fig. 1a). Thus, during the upgrade temperature phase, so-called "high pressure" phase (70 kPa for an evaporation temperature of 90°C), water vapor is produced from a waste heat source at intermediate temperature ( $T_m$  at around 90°C). This water vapor allows to realize the exothermic hydration

reaction of the reactive material at high temperature ( $T_H$ ), greater than  $T_m$ . The maximal temperature lift achieved by this system for adiabatic operation ( $\Delta T_{lift_{max}}$ ) and presented in the Clausius-Clapeyron diagram (fig. 1c), corresponds to the theoretical maximum temperature lift attainable by the salt during the temperature upgrade phase: i.e. the temperature difference between the equilibrium temperature of the salt and the evaporation temperature at the “high pressure” ( $T_{H_{max}}-T_m$ ). In real systems, a gap from this value is necessary in order to obtain a sufficient reactive power (see fig. 1d).

Once the reactive salt is fully hydrated, the charging phase (or regeneration phase) of the reactor, so-called "low pressure" phase (4 kPa for a condensation temperature of 30°C), begins. Heat at  $T_m$  (waste heat) is supplied to the reactor while it is connected to a condenser maintained at ambient temperature. As shown in fig. 1c, this temperature must be inferior to  $T_{L_{max}}$  (i.e. the condensation temperature at the “low pressure”) to allow the endothermic dehydration of the reactive solid occurs.

In order to allow to decrease the required pressure lift when high temperature lifts are sought, Goetz et al. [15] proposed a 2-salt technology, also called resorption heat pump. In this case, the evaporator and the condenser are replaced by two reactors filled with a so-called low temperature salt (see fig. 1b and d).

Thus, as shown on fig. 1b, during the charging phase waste heat at  $T_m$  is supplied to the HT reactor and the LT salt is connected to a heat sink at  $T_L$ . In order to allow simultaneously the hydration of the LT salt and the dehydration of the HT salt, the operating conditions (vapor pressure and temperature) of the LT reactor must be in the blue zone presented on fig. 1d. Therefore, this reactor has to be connected to a heat sink at  $T_L < T_{L_{max}}$  (i.e. the equilibrium pressure of the LT salt at  $T_L$  must be inferior to the equilibrium pressure of the HT salt at  $T_m$ ). In the case of  $T_L$  is higher than  $T_{L_{max}}$ , the operating conditions do not allow the hydration of the LT salt and the dehydration of the HT salt. At the end of this phase, the reactive LT salt is fully hydrated and the HT salt is fully dehydrated.

During the temperature upgrade phase, the LT reactor is connected to the waste heat at  $T_m$ . In order to achieve the dehydration of the LT reactor and the hydration of the HT reactor, the operating condition of the HT reactor must be in the orange zone of the fig. 1b, thus the HT reactor temperature must be inferior to  $T_{H_{max}}$  (i.e. the equilibrium pressure of the LT salt at  $T_m$  have to be superior to the equilibrium pressure of the HT salt at  $T_H$ ). Therefore, this phase allows to supply heat at high temperature ( $T_H$ ), and a temperature lift,  $\Delta T_{lift} = T_H - T_m$ , is obtained (see fig. 1d). Finally, at the end of this phase, the LT salt is fully dehydrated and the HT salt is fully hydrated, requiring the beginning of a new regeneration phase.

### 2.3. Proposed criteria for salt selection

From these considerations a first screening of working pairs could consist in evaluating four successive criteria:

1. a first simple criterion consists in checking whether the temperature conditions are satisfied, i.e. the hot source temperature has to be lower than the HT salt/water equilibrium temperature at high pressure ( $T_H < T_{H_{max}}$ ) and cold source temperature has to be lower than the LT salt/water equilibrium temperature at low pressure ( $T_L < T_{L_{max}}$ ) and so that reactions can occur for both LT and HT reactors.
2. The second criterion is given by the maximal temperature lift that can be reached. The maximal temperature lift is achieved for adiabatic operation and therefore corresponds to the theoretical maximum lift attainable by the HT salt during the temperature upgrade phase:  $T_{H_{max}}-T_m$ .
3. The third step consists in considering the achievable performance in terms of COP. Neglecting heat accumulation by the salts (heat capacities are low compared to reaction enthalpies) and assuming that there are no heat losses, the theoretical maximal COP of a 2-salt THT is given by:

$$COP_{max} = \frac{Q_{HT}}{Q_{m_{LT}} + Q_{m_{HT}}} = \frac{\Delta h_{r_{S_{HT}}}^0}{\Delta h_{r_{S_{HT}}}^0 + \Delta h_{r_{S_{LT}}}^0} \quad (4)$$

4. The fourth criterion is based on the necessary existence of an equilibrium drop for the thermochemical reactions to occur in finite time. This parameter influences the heat and mass transfer rates and

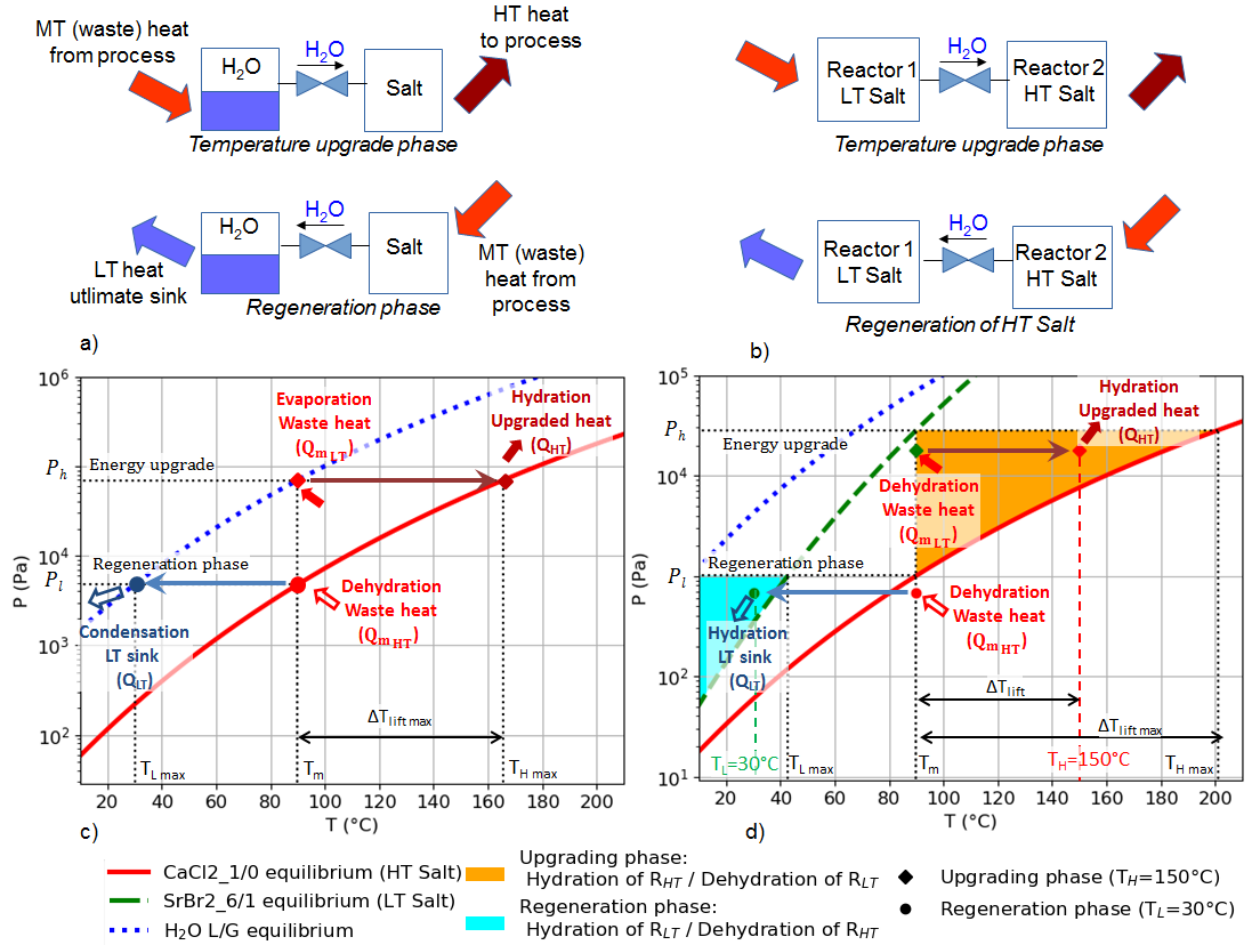


Figure 1: a) 1-salt, b) 2-salt THT working principle. c) 1-salt THT Clapeyron diagram for CaCl<sub>2</sub>/water, d) 2-salt THT Clapeyron diagram and representation of the operating areas during hydration and dehydration for CaCl<sub>2</sub>/water & SrBr<sub>2</sub>/water pairs.

therefore the reaction kinetics [16, 17]. Thus, any change in the operating temperature (*T<sub>L</sub>*, *T<sub>m</sub>* or *T<sub>H</sub>*) results in a change in the equilibrium drop and then in the reaction kinetic. However, as indicated by Obermeier et al. [17], the equilibrium drop is not an independent parameter and equal values do not produce the same heat and mass transfer rates for different reaction systems.

This parameter can be related to the chemical potential difference which represents the thermodynamic driving force of the reaction. Usually, the greater the driving force, the greater the reaction kinetic is. Under the assumptions of pure substances and ideal mixtures, the driving force can be described by the Gibbs free energy of the reaction [17]. Thus according to the eq. (2), this parameter can be written as:

$$F_m = \frac{\Delta g_r}{\nu RT} = \ln \left( \frac{p_v}{p_{eq}(T)} \right) \quad (5)$$

The vapor pressure is determined using eq. (9).

### 3. Dynamic model

Several modeling of solid/gas reactor, with different approaches (local, global) and complexity levels (1/2D, stationary/dynamic, ...) have been presented in the literature [18–20]. Most of the reported works refer to cooling or heat storage applications and only few models deal with THT applications, especially for those based on 2-salt cycles.

Thus, from modeling approaches of a solid/gas reactor developed by Lebrun et al. and Castaing-Lasvignottes et al. [18, 21], a simple and original 0D dynamic model of 2-salt THT reactor was developed by the authors [22]. It allows to study the dynamic behavior to estimate performances, mainly heating capacity, and temperature lift. The following assumptions are made:

- a Heat accumulation in the gas phase and heat losses are neglected.
- b The heat capacities are considered constant during the reaction.
- c In closed thermochemical systems (working with pure gas), the mass transfer usually does not limit reaction kinetic. Thus, the vapor pressure is assumed uniform inside the reactor.
- d The assumptions (a) and (b) imply that the salt reaction advancement ( $X_S$ ) is uniform in each reactor.  $X_S$  equals 0 at the end of the dehydration reaction (the solid is fully dehydrated) and 1 at the end of the hydration reaction (the solid is fully hydrated).
- e The kinetics of the solid/gas reactions depends only on the reaction advancement and on the equilibrium drop. This drop corresponds to the difference of the operating temperature and pressure to their value at equilibrium.
- f Uniform temperature ( $T_{SLT}$  and  $T_{SHT}$ ) and local thermal equilibrium between the gas and solid phases is assumed in the reactors.

#### 3.1. Governing Equation

##### 3.1.1. Energy balance

According to assumptions (a), (b) and (c), the energy balances of the HT and LT salt reactors are respectively written as:

$$\left[ m_{s_n} \left( 1 - (1 - X_{s_n}) \nu_{s_n} \frac{M_v}{M_{s_n}} \right) c_{s_n} + m_{exch_n} c_{exch_n} \right] \frac{dT_{s_n}}{dt} = \dot{q}_{s_n} + \dot{m}_{htfn} c_{htfn} (T_{ihtfn} - T_{ohtfn}) \quad (6)$$

with:

$$\dot{q}_{s_n} = -\dot{m}_{\nu_{s_n}} \Delta h_{r_{s_n}}^0 = \nu_{s_n} \frac{dX_{s_n}}{dt} \frac{m_{s_n}}{M_{s_n}} \Delta h_{r_{s_n}}^0 \quad (7)$$

With  $m_{s_n}$  the mass of salt n hydrated,  $\dot{m}_{\nu_{s_n}}$  the source ( $\dot{m}_{\nu_{s_n}} > 0$  in dehydration phase) or sink ( $\dot{m}_{\nu_{s_n}} < 0$  in hydration phase) of vapor due the reaction of the salt n.

##### 3.1.2. Kinetics of the solid/gas reaction

According to the assumption (e), the reaction kinetic depends on the reaction advancement and on the equilibrium drop. There are different kinetic model structures for solid-gas reaction available in the literature [20]. Arrhenius-type laws are the most frequently used. However, for reversible reactions and because of the temperature range used, Mazet et al. [23] have shown that the exponential term of the Arrhenius law can be considered as constant. Furthermore, several authors shown that the kinetic law could be written as a 1<sup>st</sup> order kinetic law for this kind of application [24–28]:

$$\frac{dX_{s_n}}{dt} = k_{cin_{s_n}} Y_{s_n} \left( 1 - \frac{p_{eq}(T_{s_n})}{p_v} \right) \quad (8)$$

where:  $Y_{s_n} = (1 - X_{s_n})$  in hydration phase and  $Y_{s_n} = X_{s_n}$  in dehydration phase.

### 3.1.3. Operating vapor pressure

The vapor operating pressure of the interconnected HT and LT reactors,  $p_v$ , is defined such as the vapor mass flow rate caught/released by the HT salt reactor is equal to the vapor mass flow rate respectively released/caught by the LT salt reactor. Thus, using Eq. (7) and Eq. (8), the vapor pressure writes:

$$p_v = \frac{A p_{eq_{s_{HT}}}(T_{s_{HT}}) - p_{eq_{s_{LT}}}(T_{s_{LT}})}{A - 1}, \text{ with } A = -\frac{m_{s_{HT}} M_{s_{LT}} \nu_{s_{HT}} k_{cin_{HT}} (1 - X_{s_{HT}})}{m_{s_{LT}} M_{s_{HT}} \nu_{s_{LT}} k_{cin_{LT}} X_{s_{LT}}} \quad (9)$$

Thus, the vapor pressure evolves between the equilibrium pressure of each reactor. This trend has been experimentally observed by [11] for a 2-salts THT using ammonia as working fluid.

Note that in case of the kinetic coefficients of both reactive salts are equals and if the salts masses are chosen in a balanced way (i.e. in a way that the overall of both reactive salts could react, cf. § 3.2.3), we have  $A = -1$ . Therefore, the operating vapor pressure is equal to the average of the equilibrium pressure of each salt.

## 3.2. Model Parameters

### 3.2.1. Reactor heat transfer coefficient (UA)

The global heat transfer coefficient of the reactor has been identified from experimental results of [10] obtained with a prototype of THT using  $\text{CaCl}_2/\text{H}_2\text{O}$  as working pair. Although UA depends on the reactor geometry and on the reactive material used, we will suppose in this paper, that the change of the reactor scale and reactive material does not affect the heat transfer characteristics. The following empirical relation of the specific heat transfer coefficient has been evaluated from hydration results:

$$\frac{UA_{S_n}}{m_{S_n}} = 131.36 e^{-3.35 X_{S_n}} \quad (10)$$

### 3.2.2. Kinetic parameter

The kinetic constant,  $k_{cin}$ , lumps the heat and mass transfers in the solid pores and the intrinsic kinetics of the reaction. It was identified thanks to the experimental reaction advancement rate obtained by Esaki et al. [10] during the hydration of a THT using  $\text{CaCl}_2$ . The best fit was found for a value of  $68 \cdot 10^{-4} \text{ s}^{-1}$  for  $k_{cin}$ .

As shown by Michel et al. [26], this value indicates that the kinetic is not the main limitation of the thermochemical reaction. In the following, this constant value of  $k_{cin}$  has been used for all the studied working pairs.

### 3.2.3. Mass of salts

In order to avoid that one of the two reactive salts limits the reaction of the other one, the mass of each salts should be chosen in a way that both reactive salts could totally react. Thus, each salt must allow to catch (respectively release) the water vapor released (respectively caught) by the other salt:

$$m_{v_{HT}} = m_{v_{LT}} \iff \nu_{s_{HT}} \frac{m_{s_{HT}}}{M_{s_{HT}}} = \nu_{s_{LT}} \frac{m_{s_{LT}}}{M_{s_{LT}}} \implies m_{s_{LT}} = m_{s_{HT}} \frac{\nu_{s_{HT}} M_{s_{LT}}}{\nu_{s_{LT}} M_{s_{HT}}} \quad (11)$$

In this study, the mass of the hydrated HT salt ( $m_{s_{HT}}$ ) has been chosen at 100 kg to get results easily scalable for industrial applications.

### 3.2.4. System control

The system is controlled using the heat transfer fluids of each reactor (LT and HT reactors). For both reactors, the heat transfer fluids inlet temperatures are fixed and are shifted at the beginning of each cycle phase. Moreover, the flow rate of the heat transfer fluid of the LT reactor ( $\dot{m}_{htf_{LT}}$ ) is set to a constant value during all the cycle. Then, the outlet temperature of the heat transfer fluid of this reactor is given by:

$$T_{o_{htf_{LT}}} = \frac{T_{i_{htf_{LT}}} - T_{S_{LT}}}{\exp\left(\frac{UA_{S_{LT}}}{\dot{m}_{htf_{LT}} c_{htf_{LT}}}\right)} + T_{S_{LT}} \quad (12)$$

For the HT reactor, during the regeneration phase the heat transfer fluid flows, with a fixed flow rate, only when the HT reactor temperature is lower than  $T_m$ . Thus, the sensible heat of the HT salt is used to start its dehydration at the beginning of the regeneration phase. In this case, the heat transfer fluid outlet temperature is calculated using equation (12).

During the temperature upgrade phase, the HT heat transfer fluid flow rate is determined in order to achieve the desired temperature difference (e.g. 5 K, 10 K, etc.) between the inlet and the outlet of the heat transfer fluid. Thus, if the salt temperature is lower than the inlet temperature of the heat transfer fluid, the heat transfer fluid does not flow; otherwise its flow rate is calculated using the following equation:

$$\dot{m}_{htf_{HT}} = \frac{-UA_{S_{HT}}}{c_{htf_{HT}} \ln\left(\frac{T_{o_{htf_{HT}}} - T_{S_{HT}}}{T_{i_{htf_{HT}}} - T_{S_{HT}}}\right)} \quad (13)$$

### 3.3. Model validation

The model has been validated using experimental results of a 1-salt THT prototype containing  $\text{CaCl}_2 \cdot 2\text{H}_2\text{O}$  as reactive pair [10]. This experimental set-up is out of the scope of this paper, and is only briefly described here. The prototype consists of a thermochemical reactor, containing a packed bed of 589 g of  $\text{CaCl}_2 \cdot 2\text{H}_2\text{O}$  placed between the plate tubes of a commercial aluminum heat exchanger. The reactor has been tested in hydration phase for an evaporator temperature of 97 °C and an inlet temperature of the heat transfer fluid of 155 °C.

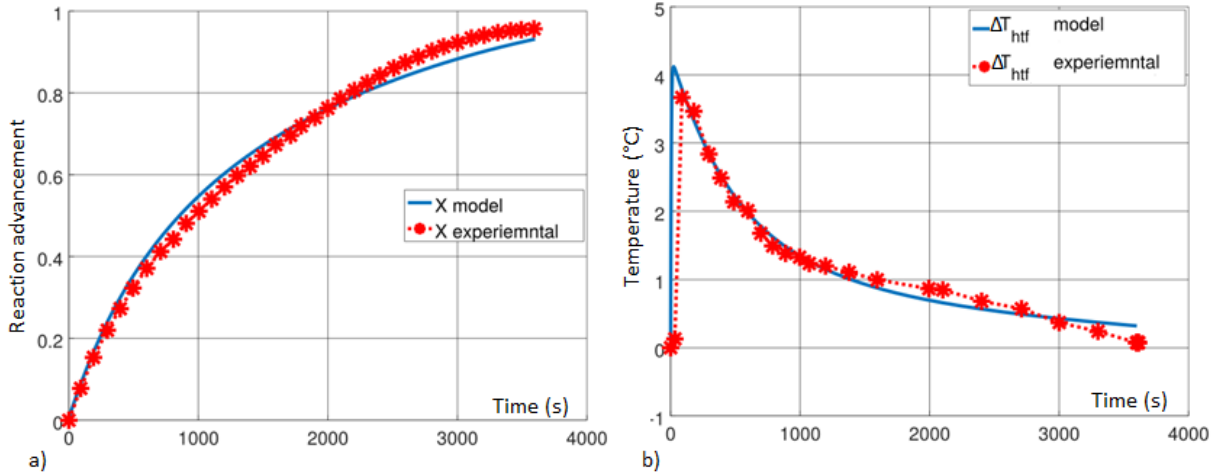


Figure 2: Experimental and simulated results of the hydration of the THT (A type reactor, Esaki et al. [10]): a) Reaction advancement vs. time during. b) Heat transfer fluid temperature difference vs. time.

As it can be seen on fig. 2, the difference between experimental and simulated results is small. The root mean square deviation is of 0.029 for the reaction advancement and of 0.82 K for the related temperature. These results demonstrate that this simple model predicts in a satisfactory way the thermal behavior of a reactor.

Note that the presented model validation will still be valid as long as the main assumptions, and especially that the mass transfer no limits the reaction, remain true. Although several authors verified this assumption [12, 26], especially for THT applications, for extreme cases, with very high heat transfer, or very low mass transfer in the reactive material, the mass transfer could become not negligible and therefore the model not valid.

In the following of this paper the identified values from the experimental results of a THT [10] (which order of magnitudes are realist) will be used to study the dynamic behavior of the THT and evaluated their performances. Furthermore, a sensitivity study of these parameters will be presented in the §5.2.1.

#### 4. Salt screening using static thermodynamic approach

In this section, the static thermodynamic approach (cf. section 2.3) is used to perform a rapid screening of available salt-H<sub>2</sub>O pairs [29, 30]. A numerical tool was developed to go through the four presented criteria. A first selection was operated by checking whether the temperature conditions are satisfied ( $T_L < T_{L_{max}}$  and  $T_H < T_{H_{max}}$ ). 77 pairs were identified from 66 initial reactions (which represents 4290 potential reactive pairs). Then criteria 2 & 3 ( $\Delta T_{max}$  and COP) were calculated and evaluated for all the 77 pairs. Finally, criteria 4 (minimal driving force) was evaluated for each promising reactive pairs.

For the sake of clarity, the work presented in this paper is focused on given heat source temperatures representative of operating conditions suitable for heat upgrading in the industry. The cold source temperature is chosen at  $T_L = 30$  °C, the waste heat temperature at  $T_m = 90$  °C and a high temperature source at  $T_H = 150$  °C.

Hence, a minimum temperature lift of 60 K is required. To take into account the necessary temperature pinches in the HT reactor for the heat transfer to occur in finite time, only pairs achieving a minimum temperature lift of 80 K are considered on fig. 3.

From these results, 21 of the 77 promising reaction couples are kept. A large discrepancy between  $\Delta T_{max}$  values is observed, from 80 K to 125 K (for the CaCl<sub>2</sub>/CuSO<sub>4</sub>/H<sub>2</sub>O pair) with a COP<sub>max</sub> ranging from 0.39 to 0.52. Besides the static thermodynamic considerations, dynamic aspects have also to be taken into account in order to estimate specific heating power.

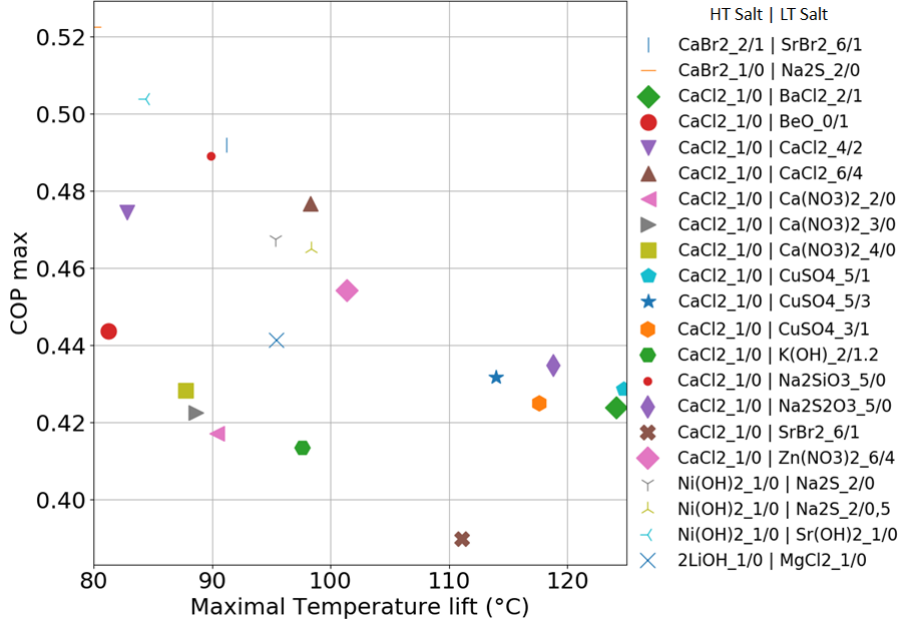


Figure 3: Maximal COP versus theoretical maximal temperature lift, for  $T_L = 30$  °C and  $T_m = 90$  °C.

fig. 4 presents a comparison of the minimal driving forces during the regeneration and the upgrading temperature phases (i.e. the minimal driving force between the hydration of the HT salt and the dehydration of the LT salt (upgrade temperature phase) vs. the minimal driving force between the hydration of the LT salt and the dehydration of the HT salt (charging phase)), for different reactive couples. Thus, reactive pairs whose the minimal driving force is for the charging phase (point under the dotted line) correspond to THT systems limited by this phase. Inversely, the upgrade temperature phase is limiting for the reactive couples situated above the dotted line.

A large discrepancy between the driving force values is observed, from 0.001 to 0.35. However, promising reactive pairs are identified, as  $\text{CaCl}_2/\text{Ca}(\text{NO}_3)_2$ ,  $\text{CaCl}_2/\text{SrBr}_2$  and  $\text{CaCl}_2/\text{K}(\text{OH})$ . They present high driving forces whose values are close between each cycle phase. This allows to avoid large reaction times gap between these phases.

## 5. Cycle performances

This part aims at analyzing the dynamic behavior and performances of a 2-salt THT. The inlet temperature of the heat transfer fluids are fixed, respectively for the LT and HT reactors, at  $T_L = 30$  °C and  $T_m = 90$  °C during the first phase and at  $T_m$  and  $T_H = 150$  °C during the temperature upgrade phase. The heat transfer fluid flow rates of the LT reactor has been chosen in order to be no limiting ( $\dot{m}_{htf_{LT}} = 1.5 \text{ kg s}^{-1}$ ) and the heat transfer fluid outlet temperature of the HT reactor ( $T_{outf_{HT}}$ ) has been set at 160 °C during the upgrading temperature phase. The corresponding temperature lift supplied by the system is 70 K. Initially, each reactor is at mid-reaction ( $X_{S_n} = 0.5$ ), the LT and HT reactors are respectively at  $T_L$  and  $T_H$ . The simulated cycle begins by the regeneration phase and is followed by the temperature upgrade phase.

To achieve continuous operation, THT system basically operates with two units of two interconnected reactors in opposite phase, each phase lasting the same time. Hence, 20 successive cycles have been simulated in order to characterize reactor behavior at cycle steady state. Moreover, cycle time is known to impact the useful heating power achievable by the system. Hence, the following results are given for the optimal cycle time at cycle steady state.

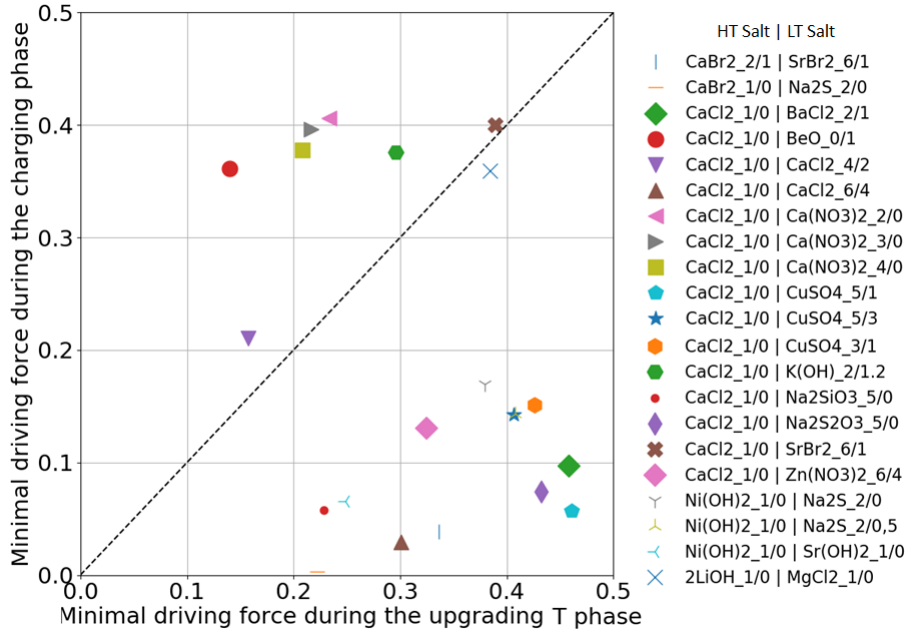


Figure 4: Minimal driving forces during the charging phase vs. during the upgrade temperature phase (for  $X_{S_n} = 0.5$ ,  $T_L = 30$  °C,  $T_m = 90$  °C and  $T_H = 150$  °C).

In order to validate the relevance of the selection criteria previously presented, two pairs, one considered as promising and the other one not selected using the salt screening, are considered:  $\langle \text{CaCl}_2 \cdot 1/2\text{H}_2\text{O} \rangle / \langle \text{SrBr}_2 \cdot 1/6\text{H}_2\text{O} \rangle$  which presents balanced driving force between LT and HT reactors and  $\langle \text{CaCl}_2 \cdot 1/2\text{H}_2\text{O} \rangle / \langle \text{BaCl}_2 \cdot 1/2\text{H}_2\text{O} \rangle$  for which the driving force during the charging step is a limiting factor (fig. 4).

### 5.1. Dynamic Behavior

The dynamic behavior of 2-salt THT using  $\langle \text{CaCl}_2 \cdot 1/2\text{H}_2\text{O} \rangle / \langle \text{SrBr}_2 \cdot 1/6\text{H}_2\text{O} \rangle$  and  $\langle \text{CaCl}_2 \cdot 1/2\text{H}_2\text{O} \rangle / \langle \text{BaCl}_2 \cdot 1/2\text{H}_2\text{O} \rangle$  reactive couples are presented fig. 5. In both cases, due to the high equilibrium drop at the beginning of each phase (due to the quick change of the imposed reactors temperatures), we observe that the thermochemical reactions are very fast. This leads to an important peak of specific heat power (defined as the power supplied/released to the heat transfer fluids of the reactor, divided by the mass of the corresponding hydrated salt) supplied/needed to the heat transfer fluid, especially for the low temperature reactor ( $>1000$  W kg<sup>-1</sup>). Because of the system control (cf. 3.2.4), this peak is lower for the high temperature reactor (112.4 W kg<sup>-1</sup> and 218.9 W kg<sup>-1</sup> respectively for the CaCl<sub>2</sub>/SrBr<sub>2</sub> and the CaCl<sub>2</sub>/BaCl<sub>2</sub> reactive pairs). In this case, the heat of reaction is first used to heat or cool the reactive solid at the desired temperature and then supplied to or taken from the heat transfer fluid. Thus, during the upgrading temperature phase, a time gap is necessary to increase the salt temperature to the desired value and to obtain upgraded heat at high temperature.

In agreement with the driving forces presented in the fig. 4, the reaction advancement evolution shows that the reaction kinetic of each phase is quite balanced for the CaCl<sub>2</sub>/SrBr<sub>2</sub> reactive pairs, while the temperature upgrade phase is much faster than the other phase for the system using the CaCl<sub>2</sub>/BaCl<sub>2</sub> couple (30 min instead of 1.5 h). In this last case, although the driving force of the upgrading temperature phase is higher than for the system using the CaCl<sub>2</sub>/SrBr<sub>2</sub> reactive pairs, lower average specific heat power of the HT reactor is obtained with during this phase: 27.1 W kg<sup>-1</sup> against 72.7 W kg<sup>-1</sup>. Hence, for the

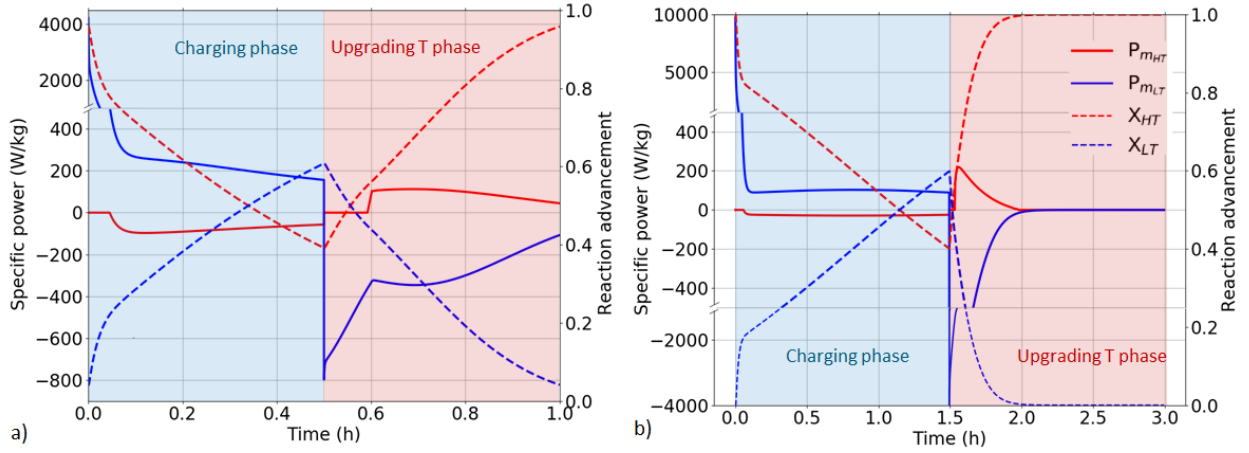


Figure 5: Specific heat power and reaction advancement versus time of 2-salt THT operating with: a)  $\langle \text{CaCl}_2 \cdot 1/2\text{H}_2\text{O} \rangle / \langle \text{SrBr}_2 \cdot 1/6\text{H}_2\text{O} \rangle$  working pairs. b)  $\langle \text{CaCl}_2 \cdot 1/2\text{H}_2\text{O} \rangle / \langle \text{BaCl}_2 \cdot 1/2\text{H}_2\text{O} \rangle$  working pairs.

$\text{CaCl}_2/\text{BaCl}_2$  pair, the system performance is therefore limited by the charging phase, especially due to the unfavorable operating conditions.

## 5.2. Kinetic reaction limitations

The THT performance directly depends to the kinetic reactions of each reactive salt. This study focuses on the relevant parameters influencing the thermochemical reaction: transfer parameters and operating conditions. Sensitivity studies allow identifying the different reactions limitations and the ways to reduce them.

### 5.2.1. Sensitivity to the transfer parameters

The sensitivity of the transfer parameters (UA and  $k_{cin}$ ) is studied for a heat transformer operating with the  $\langle \text{CaCl}_2 \cdot 1/2\text{H}_2\text{O} \rangle / \langle \text{SrBr}_2 \cdot 1/6\text{H}_2\text{O} \rangle$  working pair. Simulations have been performed for UA and  $k_{cin}$  values between 10 times and 1/10 of their respective reference value (cf. § 3.2). The average specific power released at  $T_H$  during the temperature upgrading phase for each simulation is presented in the fig. 6. It can be noticed that both transfer coefficients influence the system performances. Thus, for values lower or close to the reference value, the system performance increases significantly with the increase of the transfer coefficients. However, this impact is more pronounced for the heat transfer parameter. For example, an increase of the system specific power of respectively 48% and 12% is obtained when UA and  $k_{cin}$  are increased by a factor of two. Moreover, for transfer coefficient values superior to the reference value by five times, the kinetic parameter increase no longer impacts the system performances, unlike for the heat transfer parameter. In this case,  $k_{cin}$  no more limits the thermochemical reactions and the heat transfer becomes the main transfer limitation.

Thus, it could be interesting to intensify the heat transfer inside the reactor. Several approaches can be used as increasing the conductivity of the reactive materials, for example by adding a conductive binder as developed by several authors [31], or as coating the salt/sorbent on the surface of the reactor heat exchanger [32, 33].

### 5.2.2. Sensitivity to the operating conditions

Simulations have been performed to study the sensitivity of the driving forces. The operating temperatures directly impact the reactions equilibrium pressures (eq. (3)) and therefore the driving forces values. Thus, the sensitivity of the driving forces has been studied changing the operating temperature  $T_L$ ,  $T_H$  and

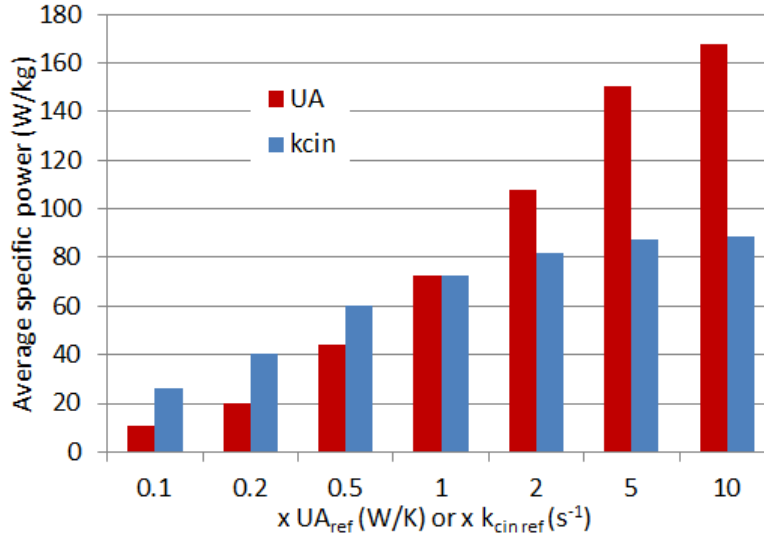


Figure 6: Influence of  $k_{cin}$  and UA on the average specific reaction power released at  $T_H$  during the temperature upgrading phase. Case of the  $\langle \text{CaCl}_2 \cdot 1/2\text{H}_2\text{O} \rangle / \langle \text{BaCl}_2 \cdot 1/2\text{H}_2\text{O} \rangle$  working pair.

$T_m$  respectively in the range 0–40 °C, 110–160 °C and 80–130 °C. Their impact to the average specific heat power released at  $T_H$  and the reaction driving forces is presented in the fig. 7.

Although the decrease of  $T_L$  (or  $T_H$ ) increases the limiting driving forces during the generation phase (upgrading temperature phase), a slight decrease in the specific power is observed. On contrary, the increase of  $T_L$  (or  $T_H$ ) leads to significantly decrease the system performance. Indeed, increasing  $T_L$  or  $T_H$  by 10 K leads to decrease the average specific power respectively by 74% and 17.8%, while decreasing these temperatures by 10 K leads to a decrease of only 19.7% and 9.1%.

As the limiting driving forces of each phase are equilibrated in the reference case, the increase of only one of these two driving forces (due to the decrease of  $T_L$  or  $T_H$ ) leads to making the other one the limiting driving force of the system. Thus, the minimal driving force of the system does not change, which does not allow to increase the average specific power. However, increasing  $T_L$  or  $T_H$  leads to decrease of the minimal driving force and therefore to decrease of the system performance. On contrary, fig. 7 shows that increasing the intermediate temperature allows to increase significantly both driving forces. Moreover, for the studied intermediate temperature range the driving forces remain equilibrated. This leads therefore to an increase of the supplied average specific heat power.

In addition to the operating temperatures, the driving forces also depend to the reactive pair. Simulations have been performed to study the impact of the reactive couples. The 21 reactive pairs selected in the §4 have been studied. In this study, the transfer and operating parameters have been set to the reference values (cf. §3.2 & §5) and only the results obtained for the optimal cycle time are presented.

fig. 8 presents the average specific power as function of the limiting driving force for these reactive pairs. Similarly to the results obtained from the sensitivity study to the operating temperatures, this figure shows that the specific heat power depends to the limiting driving force of the system. It increases linearly with the latter. The driving force is therefore an interesting parameter allowing to obtain simply an idea of the system performances. It also allows to identify the limiting phase, which is subject to the most unfavorable conditions on which it is necessary to work in priority.

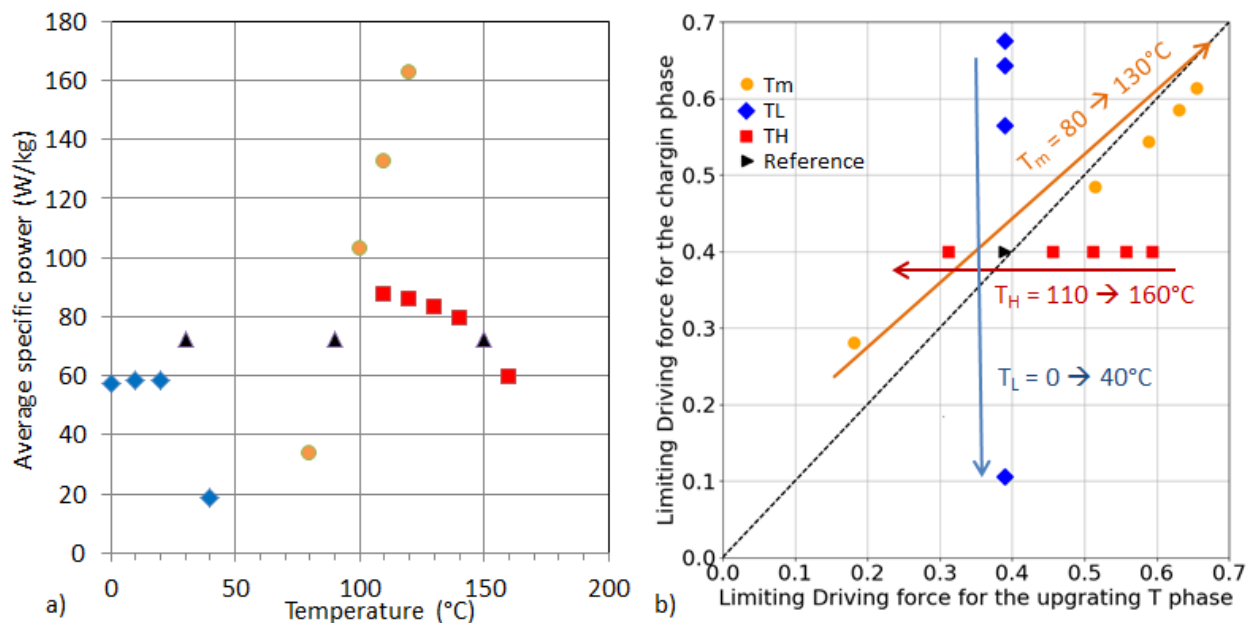


Figure 7: Impact of the operating temperatures. a) Average specific heat power released at  $T_H$  during the upgrading temperature phase. b) Evolution of the driving forces. Case of the  $\text{CaCl}_2/\text{SrBr}_2$  reactive couples.

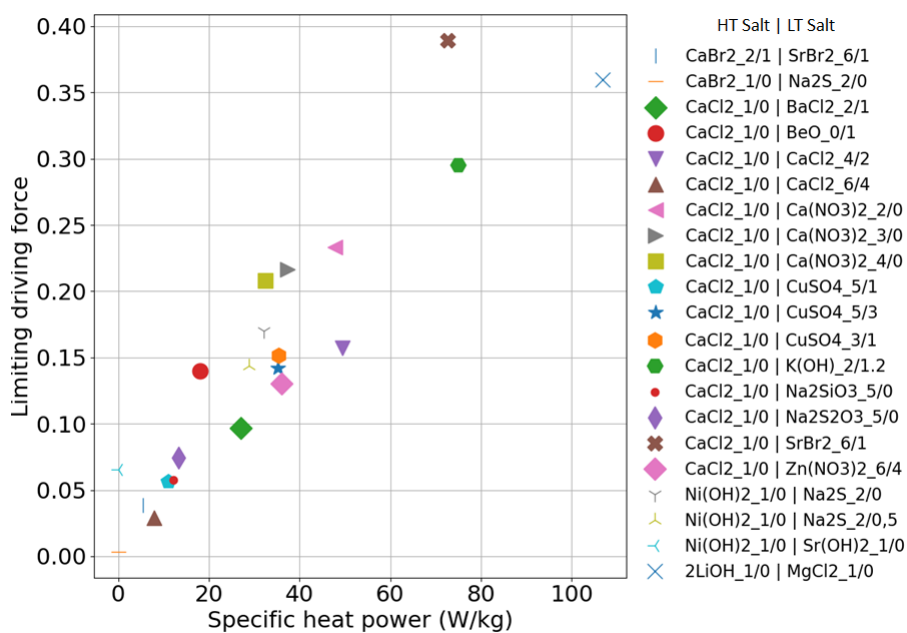


Figure 8: Limiting driving force of the system as function of the optimal average specific power for the 21 reactive pairs identified in the §2.

## 6. Conclusion

Due to the high temperature lifts obtained and the large range of operating conditions covered by the numerous reactive couples, 2-salt Thermochemical Heat Transformer process are promising systems to recover industrial waste heat by upgrading its temperature. However, the selection of best candidates for the salt pairs remains an issue today.

Hence, a four criteria methodology is proposed in this work to perform a rapid screening of salt couples and identify the best pairs for a given waste heat recovery application. The four criteria refer to comparison between source temperature and salt equilibrium temperature, COP, maximum temperature lift and driving forces.

A representative case was considered with a low temperature source at 30 °C, an intermediate at 90 °C and a high temperature source at 150 °C, pairs were discriminated using the developed tool. The first step leads to keep 77 pairs from 4290 candidates. 21 were kept considering a minimum requirement in theoretical temperature lift (>80 K). The last step allowed to identify three promising candidates:  $\text{CaCl}_2/\text{Ca}(\text{NO}_3)_2$ ,  $\text{CaCl}_2/\text{SrBr}_2$  and  $\text{CaCl}_2/\text{K}(\text{OH})$ . These reactive pairs present high and equilibrated limiting driving forces for each system cycle phase.

Cycle operation was simulated for the most promising pair ( $\text{CaCl}_2/\text{SrBr}_2$ ), using a 0D dynamic model of 2-salt THT. An average specific heating power released at high temperature as high as  $72 \text{ W kg}^{-1}$  is achieved for a temperature lift of 70 K. Secondly, kinetic reaction limitations were identified by a sensitivity study of the transfer parameters (UA and  $k_{cin}$ ) and the operating temperature. In the studied range, the increase of the heat transfer parameter play an import role on the system performances. Increasing this parameter by a factor two increases the specific power by 48%.

Finally, the significance of the driving force has been highlighted. Especially, a linear evolution of the specific heat power versus the limiting driving force has been observed. The driving force is therefore an important parameter allowing to evaluate the system performances and to identify the limiting phase, which is subject to the most unfavorable conditions on which it is necessary to act in priority.

To go further, it would be interesting to extend the proposed methodology to other working fluids (e.g. ammonia). It would be also interesting to integrate more advanced consideration on the reactor design and more specifically on the various mass or heat transfer resistances that can depend on the selected pairs: salt bulk thermophysical properties, feasibility to coat the salt on reactor heat exchanger area, material incompatibility (corrosion), etc.

## Acknowledgements

The authors wish to thank the INSA LYON (BQR FATAL RECUP) for funding this study.

## Bibliography

- [1] C. Forman, I. K. Muritala, R. Pardemann, B. Meyer, *Estimating the global waste heat potential* 57 1568–1579, 00095. doi:10.1016/j.rser.2015.12.192.  
URL <http://www.sciencedirect.com/science/article/pii/S1364032115015750>
- [2] Z. Y. Xu, R. Z. Wang, C. Yang, *Perspectives for low-temperature waste heat recovery* 176 1037–1043, 00002. doi:10.1016/j.energy.2019.04.001.  
URL <http://www.sciencedirect.com/science/article/pii/S0360544219306140>
- [3] H. Zhang, J. Baeyens, G. Cáceres, J. Degrève, Y. Lv, *Thermal energy storage: Recent developments and practical aspects* 53 1–40, 00120. doi:10.1016/j.pecs.2015.10.003.  
URL <http://www.sciencedirect.com/science/article/pii/S0360128515300149>
- [4] C. Arpagaus, F. Bless, M. Uhlmann, J. Schiffmann, S. S. Bertsch, *High temperature heat pumps: Market overview, state of the art, research status, refrigerants, and application potentials* 152 985–1010, 00000. doi:10.1016/j.energy.2018.03.166.  
URL <http://linkinghub.elsevier.com/retrieve/pii/S0360544218305759>
- [5] J. Zhang, H.-H. Zhang, Y.-L. He, W.-Q. Tao, *A comprehensive review on advances and applications of industrial heat pumps based on the practices in china* 178 800–825, 00027. doi:10.1016/j.apenergy.2016.06.049.  
URL <http://www.sciencedirect.com/science/article/pii/S0306261916308248>
- [6] K. Parham, M. Khamooshi, D. B. K. Tematio, M. Yari, U. Atikol, *Absorption heat transformers – a comprehensive review* 34 430–452, 00000. doi:10.1016/j.rser.2014.03.036.  
URL <http://www.sciencedirect.com/science/article/pii/S136403211400197X>

- [7] L. L. Vasiliev, D. A. Mishkinis, A. A. Antukh, A. G. Kulakov, L. L. Vasiliev, Resorption heat pump 24 (13) 1893–1903, 00079. doi:10.1016/j.applthermaleng.2003.12.018.  
URL <http://www.sciencedirect.com/science/article/pii/S1359431104000079>
- [8] Y. Q. Yu, P. Zhang, J. Y. Wu, R. Z. Wang, Energy upgrading by solid–gas reaction heat transformer: A critical review 12 (5) 1302–1324, 00000. doi:10.1016/j.rser.2007.01.010.  
URL <http://www.sciencedirect.com/science/article/pii/S1364032107000299>
- [9] S. Wu, T. Li, T. Yan, R. Wang, Experimental investigation on a novel solid-gas thermochemical sorption heat transformer for energy upgrade with a large temperature lift 148 330–338, 00000. doi:10.1016/j.enconman.2017.05.041.  
URL <http://linkinghub.elsevier.com/retrieve/pii/S0196890417304843>
- [10] T. Esaki, M. Yasuda, N. Kobayashi, Experimental evaluation of the heat output/input and coefficient of performance characteristics of a chemical heat pump in the heat upgrading cycle of CaCl<sub>2</sub> hydration 150 365–374, 00000. doi:10.1016/j.enconman.2017.08.013.  
URL <http://linkinghub.elsevier.com/retrieve/pii/S0196890417307239>
- [11] S. Wu, T. Li, T. Yan, R. Wang, Advanced thermochemical resorption heat transformer for high-efficiency energy storage and heat transformation 175 1222–1233, 00001. doi:10.1016/j.energy.2019.03.159.  
URL <https://www.sciencedirect.com/science/article/pii/S0360544219305791>
- [12] M. Richter, M. Bouché, M. Linder, Heat transformation based on CaCl<sub>2</sub>/h<sub>2</sub>O – part a: Closed operation principle 102 615–621, 00010. doi:10.1016/j.applthermaleng.2016.03.076.  
URL <http://www.sciencedirect.com/science/article/pii/S1359431116303696>
- [13] M. Richter, E.-M. Habermann, E. Siebecke, M. Linder, A systematic screening of salt hydrates as materials for a thermochemical heat transformer 659 136–150, 00010. doi:10.1016/j.tca.2017.06.011.  
URL <https://linkinghub.elsevier.com/retrieve/pii/S0040603117301557>
- [14] T. Li, R. Wang, J. K. Kiplagat, A target-oriented solid-gas thermochemical sorption heat transformer for integrated energy storage and energy upgrade 59 (4) 1334–1347, 00032. doi:10.1002/aic.13899.  
URL <http://doi.wiley.com/10.1002/aic.13899>
- [15] V. Goetz, F. Elie, B. Spinner, The structure and performance of single effect solid-gas chemical heat pumps 13 (1) 79–96, 00000. doi:10.1016/0890-4332(93)90027-S.  
URL <http://www.sciencedirect.com/science/article/pii/089043329390027S>
- [16] N. Mazet, H.-B. Lu, Improving the performance of the reactor under unfavourable operating conditions of low pressure 18 (9) 819–835, 00000. doi:10.1016/S1359-4311(97)00108-7.  
URL <http://www.sciencedirect.com/science/article/pii/S1359431197001087>
- [17] J. Obermeier, K. Müller, W. Arlt, Thermodynamic analysis of chemical heat pumps 88 489–496, 00008. doi:10.1016/j.energy.2015.05.076.  
URL <https://linkinghub.elsevier.com/retrieve/pii/S036054421500657X>
- [18] J. Castaing-Lasvignottes, P. Neveu, Development of a numerical sizing tool applied to a solid-gas thermochemical transformer—II. influence of external couplings on the dynamic behaviour of a solid-gas thermochemical transformer 17 (6) 519–536, 00000. doi:10.1016/S1359-4311(96)00066-X.  
URL <http://www.sciencedirect.com/science/article/pii/S135943119600066X>
- [19] F. Marias, P. Neveu, G. Tanguy, P. Papillon, Thermodynamic analysis and experimental study of solid/gas reactor operating in open mode 00000. doi:10.1016/j.energy.2014.01.101.  
URL <http://www.sciencedirect.com/science/article/pii/S0360544214001236>
- [20] T. Nagel, S. Beckert, C. Lehmann, R. Gläser, O. Kolditz, Multi-physical continuum models of thermochemical heat storage and transformation in porous media and powder beds—a review 178 323–345, 00016. doi:10.1016/j.apenergy.2016.06.051.  
URL <http://www.sciencedirect.com/science/article/pii/S0306261916308261>
- [21] M. Lebrun, B. Spinner, Models of heat and mass transfers in solid–gas reactors used as chemical heat pumps 45 (7) 1743–1753, 00057. doi:10.1016/0009-2509(90)87052-T.  
URL <http://linkinghub.elsevier.com/retrieve/pii/000925099087052T>
- [22] B. Michel, M. Clause, Thermochemical heat transformer for waste heat recovery: consideration of dynamic aspects for design, in: ICR 2019, p. 8, 00000.
- [23] N. Mazet, M. Amouroux, B. Spinner, Analysis and experimental study of the transformation of a non-isothermal solid/gas reacting medium 99 (1) 155–174, 00000. doi:10.1080/00986449108911585.  
URL <http://www.tandfonline.com/doi/abs/10.1080/00986449108911585>
- [24] P. Neveu, J. Castaing-Lasvignottes, Development of a numerical sizing tool for a solid-gas thermochemical transformer—i. impact of the microscopic process on the dynamic behaviour of a solid-gas reactor 1800000.
- [25] S. Dutour, N. Mazet, J. Joly, V. Platel, Modeling of heat and mass transfer coupling with gas–solid reaction in a sorption heat pump cooled by a two-phase closed thermosyphon 60 (15) 4093–4104, 00018. doi:10.1016/j.ces.2005.02.046.  
URL <https://linkinghub.elsevier.com/retrieve/pii/S0009250905001570>
- [26] B. Michel, P. Neveu, N. Mazet, Comparison of closed and open thermochemical processes, for long-term thermal energy storage applications 72 702–716, 00000. doi:10.1016/j.energy.2014.05.097.  
URL <http://www.sciencedirect.com/science/article/pii/S0360544214006641>
- [27] L. Farcot, N. Le Pierrès, B. Michel, J.-F. Fourmigué, P. Papillon, Numerical investigations of a continuous thermochemical heat storage reactor 20 109–119, 00000. doi:10.1016/j.est.2018.08.020.  
URL <http://www.sciencedirect.com/science/article/pii/S2352152X18301774>
- [28] A. Fopah Lele, F. Kuznik, H. U. Rammelberg, T. Schmidt, W. K. L. Ruck, Thermal decomposition kinetic of salt hydrates

- for heat storage systems 154 447–458, 00000. doi:10.1016/j.apenergy.2015.02.011.  
URL <http://www.sciencedirect.com/science/article/pii/S0306261915001828>
- [29] K. E. N'Tsoukpoe, T. Schmidt, H. U. Rammelberg, B. A. Watts, W. K. L. Ruck, A systematic multi-step screening of numerous salt hydrates for low temperature thermochemical energy storage 124 1–16, 00000. doi:10.1016/j.apenergy.2014.02.053.  
URL <http://www.sciencedirect.com/science/article/pii/S0306261914001974>
- [30] K. Visscher, J. Veldhuis, H. Oonk, P. an Ekeren, J. Blok, Compacte chemische seizoenopslag van zonnearmte, 00000.
- [31] J. Cot-Gores, A. Castell, L. F. Cabeza, Thermochemical energy storage and conversion: A-state-of-the-art review of the experimental research under practical conditions 16 (7) 5207–5224, 00159. doi:10.1016/j.rser.2012.04.007.  
URL <http://www.sciencedirect.com/science/article/pii/S1364032112002651>
- [32] L. Calabrese, L. Bonaccorsi, P. Bruzzaniti, E. Proverbio, A. Freni, SAPO-34 based zeolite coatings for adsorption heat pumps 187 115981, 00000. doi:10.1016/j.energy.2019.115981.  
URL <http://www.sciencedirect.com/science/article/pii/S0360544219316755>
- [33] L. Schnabel, M. Tatlier, F. Schmidt, A. Erdem-Şenatalar, Adsorption kinetics of zeolite coatings directly crystallized on metal supports for heat pump applications (adsorption kinetics of zeolite coatings) 30 (11) 1409–1416, 00045. doi:10.1016/j.applthermaleng.2010.02.030.  
URL <http://www.sciencedirect.com/science/article/pii/S1359431110001079>